

A Compact Ultra-Wideband Antenna for Time- and Frequency-Domain Applications

Nader Behdad* and Kamal Sarabandi

Department of Electrical Engineering and Computer Science
University of Michigan, Ann Arbor, MI, 48109-2122
behdad@eecs.umich.edu, saraband@eecs.umich.edu

1. INTRODUCTION

A few decades after the early investigations on ultra-wideband (UWB) wireless systems, they have found a wide range of applications including ground penetrating radars, high data rate short range wireless local area networks, communication systems for military, and UWB short pulse radars for automotive and robotics applications to name a few [1-3]. Such systems require antennas that are able to operate across a very large bandwidth with consistent polarization and radiation patterns parameters over the entire band.

In this paper, a new type of single-element wideband antenna is proposed that can provide wide bandwidth and consistent polarization over the frequency range that the antenna is impedance matched. The antenna is composed of two parallel sectorial loop antennas (SLAs) that are connected along an axis of symmetry. The geometrical parameters of this antenna are experimentally optimized and it is shown that the antenna can easily provide a wideband impedance match over an 8.5:1 frequency range. The gain and radiation patterns across the frequency range of operation remain almost constant particularly over the first two octaves of its impedance bandwidth. The antenna geometry is then modified in order to reduce its size and weight without compromising its bandwidth. This helps fabrication and installation of the antenna operating for lower frequency applications such as ground penetrating radars or broadcast television where the physical size of the antenna is large.

2. ANTENNA DESIGN

The topology of the proposed antenna is shown in Fig. 1(b). The antenna is composed of two sectorial loop antennas, as shown in Fig. 1(a), which are connected in parallel along its vertical axis of symmetry. The inner and outer radii of the loop R_{in} and R_{out} and the sector angle, α , are the three parameters which completely determine the geometry of the antenna and hence its frequency response. The lowest frequency of operation of the SLA, shown in Fig. 1(a), is determined by the overall effective circumference of the loop as expressed by the following approximate formula:

$$f_l = \frac{2c}{(\pi - \alpha + 2)\sqrt{\epsilon_{eff}}(R_{in} + R_{out})} \quad (1)$$

where ϵ_{eff} is the effective dielectric constant of the antenna's surrounding medium and c is the speed of light. The average radius of the loop, $R_{av}=(R_{in}+R_{out})/2$, is determined using (1). Therefore, the only geometrical parameters that remain to be optimized are α and $\tau=(R_{out}-R_{in})$. In order to obtain the optimum value of α , nine different antennas with $R_{in}=13\text{mm}$ and $R_{out}=14\text{mm}$ and α values from 5° up to 80° were simulated using a FDTD based simulation software. The antennas were then fabricated and their responses were measured. Since the antenna topology shown in Figure 1 needs a balanced feed, half of the structure over a ground plane is used and a simple coaxial probe is used to feed it (as shown in Fig. 3). For simplicity in the fabrication process, the antenna is printed on a thin

$3 \times 1.5 \text{ cm}^2$ dielectric substrate with dielectric constant of $\epsilon_r=3.4$ and thickness of 0.5 mm and is mounted on a $10 \text{ cm} \times 10 \text{ cm}$ ground plane.

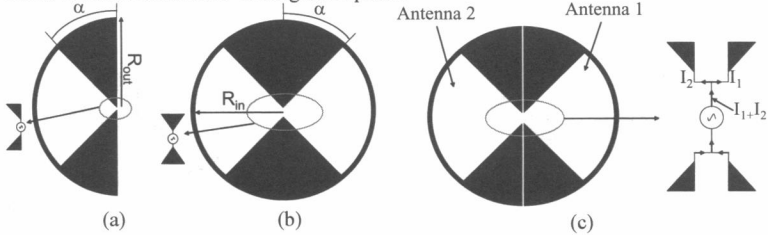


Fig. 1. (a) Geometry of the sectorial loop antenna, (b) coupled sectorial loop antenna, and (c) its feeding network.

For brevity, only the measured S_{11} values for the antennas with $\alpha=5^\circ, 20^\circ, 40^\circ, 60^\circ, 80^\circ$ are presented in Figure 2(a). It is seen that as α increases from 5° to 90° the impedance bandwidth of the antenna increases and reaches its maximum for $\alpha=60^\circ$ with an impedance bandwidth from 3.7 GHz to 10 GHz . The next step in the experimental optimization is to find the optimum τ value. For doing so, three different antennas with $\alpha=60^\circ, R_{av}=13.5 \text{ mm}$, and $\tau=0.4, 1.0,$ and 1.6 mm are simulated fabricated and the measured S_{11} of these antennas are shown in Figure 3(b). It is observed that as τ is decreased, the antenna bandwidth increases. This provides a method for designing CSLAs with very large bandwidth.

It is possible to scale the dimensions of the CSLA such that it operates at lower frequencies for applications such as TV broadcasting or ground-penetrating radars. For these applications the wavelength is large, therefore the antenna dimensions become very large. This increases the antenna weight and its wind resistance; therefore, it is desirable to reduce the metallic surface of the antenna as much as possible, while maintaining its wideband characteristics. In order to do this, one must note that the electric current density on the antenna surface is very large around the antenna's edges and sharp corners. Examining the electric current density on the surface of the antenna using the method of moments also confirms that magnitude of the electric current density is very small in the sector confined in the range of $-30^\circ \leq \theta \leq 30^\circ$ and much larger along the edges and sharp corners. This suggests that this sector of the antenna can be removed without significantly disturbing the current distribution on its surface.

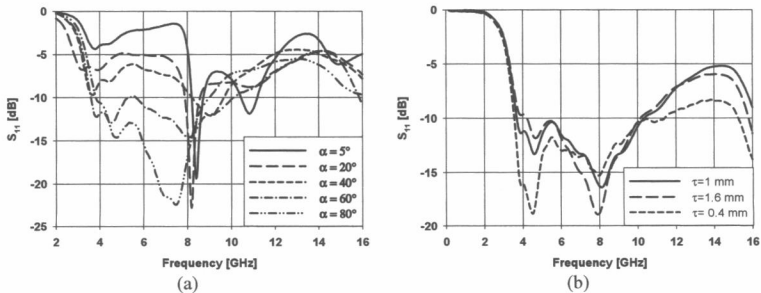


Fig. 2. Measured S_{11} of CSLAs with $R_{av}=13.5 \text{ mm}$, $\tau=1 \text{ mm}$. (a) different α values with $\tau=1 \text{ mm}$ and (b) $\alpha=60^\circ$ with different τ values.

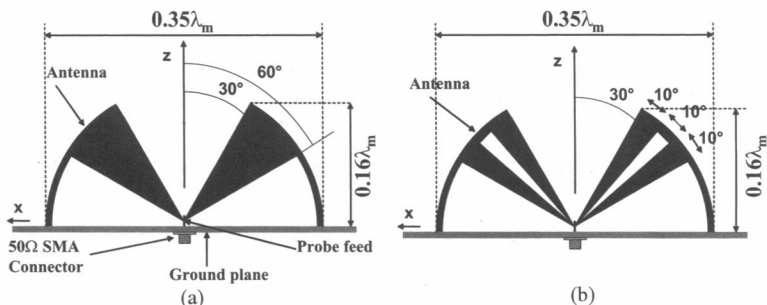


Fig. 3. Geometry of the modified CSLAs. (a) M1-CSLA and (b) M2-CSLA

The topology of this antenna is shown in Fig. 3(a) and it is called the M1-CSLA. Examining the current distribution of the M1-CSLA, it is found out that another sector from the middle of the M1-CSLA can also be removed without significantly disturbing the current distribution on the surface of the antenna. This antenna is shown in Fig. 3(b) and is called the M2-CSLA.

3. RESULTS AND DISCUSSION

Using the procedure described above, three different (original, M1-, and M2-) CSLAs were designed, fabricated, and tested. The antennas have $R_{av}=27.9\text{mm}$, $\alpha=60^\circ$, and $\tau=0.2\text{mm}$ and are fabricated on a $6\times 3\text{cm}^2$ substrate with dielectric constant of $\epsilon_r=3.4$. They are then mounted on a $20\times 20\text{cm}^2$ ground plane and fed with a coaxial probe. The measured S_{11} of these antennas are shown in Fig. 4. It is seen that the three antennas have a VSWR less than 2 over an 8.5:1 bandwidth (1.7 GHz- 14.5 GHz). The radiation patterns of the original CSLA and M2-CSLA are measured at nine different frequencies from 2GHz to 16GHz. It is observed that the radiation patterns remain consistent as the frequency increases from 2GHz to 8GHz. As frequency is increased beyond 8GHz, however, the patterns start to change. This is the result of the much larger electrical dimensions of the antenna at higher frequencies. However, the antenna has excellent match and consistent radiation parameters over, at least, two octaves of bandwidth, which is enough for most UWB systems.

In addition to the frequency-domain responses, the time-domain characteristics of the antennas must also be examined. In order to do this, the measurement setup shown in Fig. 5 is used. In this case, two identical CSLAs, of different types, are placed 30cm apart in a small anechoic chamber and are connected to the two ports of a calibrated HP8720D vector network analyzer (VNA) outside of the chamber. The VNA is then used to measure the wideband (2GHz-14GHz) transmission coefficient (S_{21}) of this system in frequency domain. It then calculates the time-domain S_{21} from the measured coherent frequency-domain data by taking its inverse Fourier transform. The time domain impulse responses of the system consisting of two original, M1-, and M2-, CSLAs are shown in Fig. 6. In this figure, the time-domain impulse response of a system consisting of a coaxial cable with the same electrical length is also presented. Since the impulse response of the cable should ideally be a delta function, this can be used as a means for comparing the time domain responses of the antennas. It is observed that the original CSLA has the least distortion and the magnitudes of the multiple reflections that follow the main pulse are lower than the other two antennas. On the other hand, the M2-CSLA has the worst

time-domain response of the three and has stronger multiple reflections. This is attributed to the increased number of discontinuities in the antenna surface. These cause multiple reflections of a time-domain pulse and distort the antenna response. In order to observe this more clearly, the time domain S_{11} of the three antennas are shown in Fig. 7. As is seen from this figure, the minor reflections in the M2-CSLA are much stronger and occur more than the other two antennas. Nevertheless, as Fig.6 shows, the magnitudes of the minor reflections are all 30dB or more below the main received pulse.

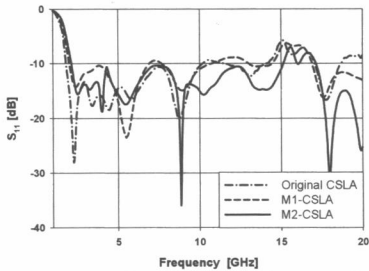


Fig. 4. Measured S_{11} of the original-, M1-, and M2-CSLAs. ($R_{av}=27.9\text{mm}$, $\alpha=60^\circ$, $\tau=0.2\text{ mm}$)

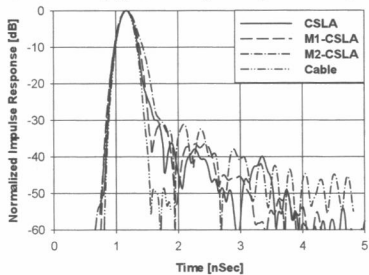


Fig. 6. Measured time-domain impulse response (S_{21}) of different CSLAs.

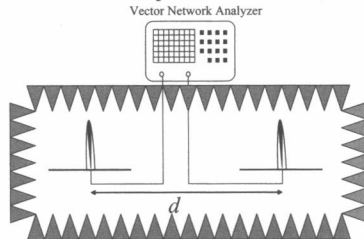


Fig. 5. The proposed setup for measuring the time-domain characteristics of the CSLAs. $d=30\text{cm}$ and the antennas are identical.

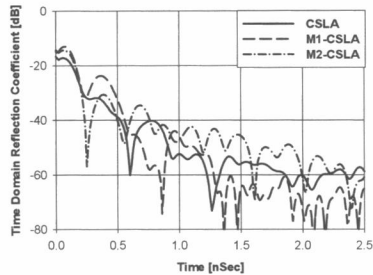


Fig. 7. Time-domain S_{11} of different CSLA types measured with a calibrated VNA.

4. CONCLUSIONS

A novel ultra-wideband coupled sectorial loop antenna is designed that has an 8.5:1 impedance bandwidth. The antenna has consistent radiation parameters over a 4:1 frequency range with excellent polarization purity over the entire 8.5:1 frequency range. Modified versions of this UWB antenna, with reduced metallic surfaces and similar radiation parameters, were also designed, fabricated, and measured. Measurement results indicate that these modifications do not adversely affect the UWB behavior of the antenna.

5. REFERENCES

- [1] C. A. Balanis, "Antenna Theory: Analysis and Design", Wiley, 2nd Edition, 1996.
- [2] Y. Mushiake, "Self-Complementary Antennas: Principle of Self-Complementarity for Constant Impedance", Springer, 1996.
- [3] G. Kumar and K. Ray, "Broadband Microstrip Antennas", Artech House, 2003, Norwood, MA.